International Journal of
Molecular Sciences

MDPI

Article

ns-μs Time-Resolved Step-Scan FTIR of ba_3 Oxidoreductase from *Thermus thermophilus*: Protonic Connectivity of w941-w946-w927

Antonis Nicolaides [1], Tewfik Soulimane [2] and Constantinos Varotsis [1,*]

[1] Department of Environmental Science and Technology, Cyprus University of Technology, P.O. Box 50329, 3603 Lemesos, Cyprus; ag.nicolaides@edu.cut.ac.cy
[2] Chemical and Environmental Science Department and Materials & Surface Science Institute, University of Limerick, V94 T9PX Limerick, Ireland; tewfik.soulimane@ul.ie
* Correspondence: c.varotsis@cut.ac.cy; Tel.: +357-2500-2451

Academic Editor: Samuel De Visser
Received: 15 August 2016; Accepted: 21 September 2016; Published: 29 September 2016

Abstract: Time-resolved step-scan FTIR spectroscopy has been employed to probe the dynamics of the ba_3 oxidoreductase from *Thermus thermophilus* in the ns-μs time range and in the pH/pD 6–9 range. The data revealed a pH/pD sensitivity of the D372 residue and of the ring-A propionate of heme a_3. Based on the observed transient changes a model in which the protonic connectivity of w941-w946-927 to the D372 and the ring-A propionate of heme a_3 is described.

Keywords: cytochrome ba_3; ns time-resolved step-scan FTIR; heme-copper oxidoreductases

1. Introduction

The electron and proton transfers in conjunction with the protonic connectivity between the environments sensed by key residues play a vital role in the biological function of proteins [1]. The conformational rigidity of *Thermophilic* enzymes against heat denaturation has attracted the biotechnological research community because of the molecular events associated with enzymatic catalysis. Based on the crystal structure cytochrome ba_3 from *Thermus thermophilus* contains a homodinuclear copper center (Cu_A), a low-spin heme *b*, and a heme a_3-Cu_B center [2–24]. Cytochrome ba_3 catalyzes the reductions of oxygen (O_2) to water (H_2O) and of nitric oxide (NO) to nitrous oxide (N_2O), as well and the oxidation of carbon monoxide (CO) to carbon dioxide (CO_2) [2–24]. The photolyzed ba_3-CO species is an excellent model for time-resolved spectroscopic studies [7–9,13,15,18,24]. In the past, we used time-resolved Raman and step-scan FTIR (TRS^2-FTIR) spectroscopy to probe the binding of CO to Cu_B and the structural changes of the ring-A propionate of heme a_3 and D372 [7–10]. It was concluded that the *trans*/*cis* isomerization of the ring-D propionate plays a crucial role in controlling the orientations of "docked" CO between the heme rings-A and -D propionates and that the protein environment removes the barrier to the two orientations of CO [10]. The role of the heme a_3-D372-H_2O site and of ring-A propionate as proton carriers to the H_2O pool, which is conserved among all structurally-known heme-copper oxidases, were reported [11,16,18,23]. The observation of deprotonated and protonated forms of heme a_3 rings-A and -D propionate and D372 indicated a protonic connectivity between the ring-A propionate, a H_2O molecule and D372. It was proposed that the environment of the ring-A heme a_3 propionate-D372-H_2O moiety can contribute to proton motion [18,23].

Time-resolved Raman and step-scan FTIR are powerful structure-sensitive techniques for exploring changes that occur to metal centers and individual amino acids as a result of changes in the ligation state of the metal centers and/or redox and conformational changes induced by

the changes in the coordination of the metal centers [24–27]. The temperature dependency of these changes is expected to give insight into the thermostability of the thermophilic enzymes. Ligand photodissociation can also induce protonation/deprotonation reactions of key residues and the pH dependency of the photodynamic/protonation/deprotonation can contribute towards the elucidation of events not previously reached by other spectroscopic techniques. Furthermore, the detection of protonation/deprotonation of ionizable groups is important towards the elucidation of the proton motions that take place in cytochrome c oxidases. The dynamics of the protein cavities in controlling the motion of O_2 migration to the binuclear heme Fe-Cu_B center is also important towards the elucidation of ligand binding since the enzyme operates at high temperature/low O_2 concentration. To address these issues the Time Resolved Step-Scan Fourier Transform Infrared (TRS^2-FTIR) studies of the fully-reduced CO complex in the pH/pD 6–9 range were examined and compared to determine the conformations of the key residue D372 and those of the heme a_3 ring-A propionate. The main goal was to compare the pH/pD results in a time-resolved approach for the protonated and deprotonated forms of ba_3. The effect of H/D exchange and the dynamic behavior of the 1749/1743 and 1723 cm^{-1} modes which have been assigned to ν(COO(H)) of two conformations of the protonated forms of D372, as well as the coupling of the protonic connectivity of w941-w946-w927 to the ring-A propionate of heme a_3 and D372 are discussed.

2. Results

Figure 1 shows the Time Resolved Step-Scan Fourier Transform Infrared (TRS^2-FTIR) difference spectra (t_d = 100–80,000 ns, 4 cm^{-1} spectral resolution) of fully-reduced ba_3-CO at pH 7.0 subsequent to CO photolysis by a 7 ns 532 nm laser pulse. At t_d = 100 ns, the spectra show a peak at 1697 cm^{-1}, "W" shape troughs at 1706 and 1724 cm^{-1}, and also features at 1717(+), 1733(+), 1738 (−), 1744(−), and 1749(+) cm^{-1}. The peak/trough at 1697/1706 cm^{-1} is characteristic of the perturbation of the C=O stretching band exhibiting stronger H-bonding interaction to surrounding groups in the transient spectra that we have assigned to the ring-A propionate of heme a_3. [7]. At t_d = 500–80,000 ns the 1706 cm^{-1} mode appears as a doublet with intensity and frequency changes. The 1717 and 1733 cm^{-1} modes, which are not exhibiting frequency shifts or intensity changes in the t_d = 100–80,000 ns range, can be attributed to the C=O mode of either protonated aspartic or glutamic residues which are affected by the induced perturbation of CO photodissociation. The 1749/1738, 1744 cm^{-1} modes have been tentatively assigned to the ν(COO(H)) of two conformations of protonated D372 [7,18]. A broad negative mode at 1548 cm^{-1} is also shown and is tentatively assigned, in agreement with previous work, to originate from the coupled His-Tyr ring mode with large contributions from the C–N of the covalent bond between both ring systems [28]. The 1541 cm^{-1} positive mode appeared as a broad peak and it was attributed to amide II vibrations and remained unchanged in the t_d = 100–80,000 ns range [29]. Features consisting of a negative peak at 1530 and positive peak at 1559 cm^{-1} are present at t_d = 100 ns, and were previously assigned to the $\nu_{as}(COO^-)$ of the deprotonated form of the ring-A propionate of heme a_3 [11,18,23]. This is evidence that there is equilibrium between the protonated and deprotonated forms of the ring-A propionate of heme a_3. It should be noted that the transient binding of CO to Cu_B in aa_3 oxidase is dynamically linked to structural changes around a protonated carboxyl group [30]. Finally, a peak/trough at 1506/1513 cm^{-1} is present and exhibits small intensity changes, but the ratio of the 1506/1513 cm^{-1} modes remained unchanged. This derivative form feature has been attributed to tyrosinate/tyrosine vibrations [31].

Figure 2 shows the Time Resolved Step-Scan Fourier Transform Infrared (TRS^2-FTIR) difference spectra of 1500–1760 cm^{-1} region (t_d = 100–80,000 ns, 4 cm^{-1} spectral resolution) of fully-reduced ba_3-CO at pH 6.0 subsequent to CO photolysis by a 7 ns 532 nm laser pulse. The Time Resolved Step-Scan (TRS^2) FTIR difference spectra in the 1690–1760 cm^{-1} region show the following changes when compared with those obtained at pH 7. At t_d = 100 ns, the protonated form of D372 is observed at 1742 cm^{-1}, showing a 7 cm^{-1} downshift, which is representative of a weaker C=O bond exhibiting stronger H-bonding interaction to surrounding groups. The 1733 cm^{-1} mode has gained intensity,

whereas that of the 1717 cm^{-1} remained the same. The 1697 cm^{-1} mode is not altered in intensity and/or frequency shifts; however, there are two weak negative peaks located at 1706 and 1714 cm^{-1}, which at t_d = 80,000 ns have gained intensity and appeared as a single mode at 1714 cm^{-1}. Compared to pH 7, we conclude that there is a pH sensitivity of the protonated forms of D372 and the ring-A propionate of heme a_3. The observed 1728(−), 1733(+), and 1742(+) cm^{-1} modes do not present any intensity changes or frequency shifts in the t_d = 100–80,000 ns range. Compared to the pH 7 spectra, there is also a frequency shift of the 1723 cm^{-1} mode, which has been attributed to one of the two conformations of D372, to 1728 cm^{-1}. This indicates sensitivity upon protonation of the second conformer of D372. The 1559 cm^{-1} mode is broader and the 1541 cm^{-1} mode at pH 6 is similar to that at pH 7. The negative peak at 1548 cm^{-1} observed at pH 7, becomes a doublet with the appearance of a new negative peak at 1554 cm^{-1}. The trough at 1530 cm^{-1}, which was previously assigned to the deprotonated form of $\nu_{as}(COO^-)$ of the ring-A propionate of heme a_3, is present at pH 6 without presenting any changes regarded to the pH alteration.

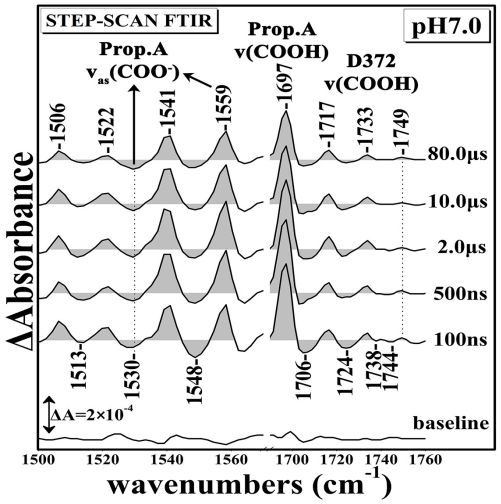

Figure 1. Time Resolved Step-Scan Fourier Transform Infrared (TRS^2-FTIR) difference spectra of 1500–1760 cm^{-1} region (t_d = 100–80,000 ns, 4 cm^{-1} spectral resolution) of fully-reduced ba_3-CO subsequent to CO photolysis by a 7 ns 532 nm laser pulse at pH 7.0.

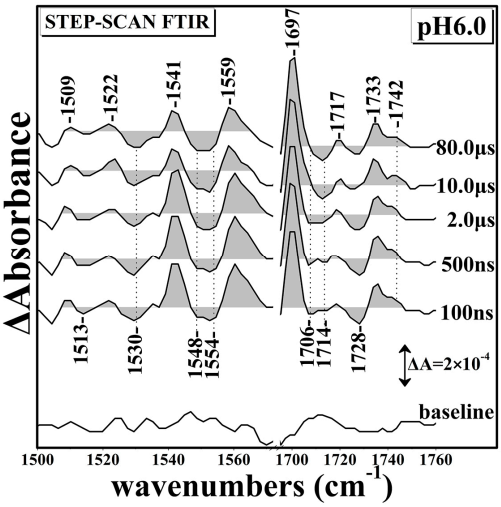

Figure 2. Time Resolved Step-Scan Fourier Transform Infrared (TRS^2-FTIR) difference spectra of 1500–1760 cm^{-1} region (t_d = 100–80,000 ns, 4 cm^{-1} spectral resolution) of fully-reduced ba_3-CO subsequent to CO photolysis by a 7 ns 532 nm laser pulse at pH 6.0.

Figure 3 shows the Time Resolved Step-Scan Fourier Transform Infrared (TRS^2-FTIR) difference spectra of 1500–1760 cm^{-1} region (t_d = 100–80,000 ns, 4 cm^{-1} spectral resolution) of fully-reduced ba_3-CO at pH 9.0 subsequent to CO photolysis by a 7 ns 532 nm laser pulse. At t_d = 100 ns, the observed peak/trough feature of 1697/1706 cm^{-1} is similar to that observed at pH 7. This is in contrast to the pH 6 data where two negative peaks at 1706 and 1714 cm^{-1} were observed indicating the pH sensitivity of the ring-A propionate of heme a_3. The protonated form of D372 observed at 1749 cm^{-1} exhibits a 7 cm^{-1} upshift when compared with that observed at pH 6, and a 3 cm^{-1} downshift when compared with that observed at pH 7, confirming the pH sensitivity of the protonated D372. In addition, the negative peak at 1739 cm^{-1}, which has been assigned to D372, has gained intensity at t_d = 100 ns when compared to that at pH 9, but at t_d = 80 µs has lost almost all of its intensity. This observation indicates that the dynamics of the D372 are linked to the dynamics of the photodissociated CO [7,23]. The deprotonated forms of the ring-A propionate exhibit significant changes as the 1530 cm^{-1} mode appears as a doublet. In addition, at t_d = 100 ns, there are two trough at 1548 and 1554 cm^{-1}. The latter trough loses intensity at times longer than 100 ns and disappears at t_d = 80 µs, indicating that its behavior is coupled to that of the 1739 cm^{-1} trough.

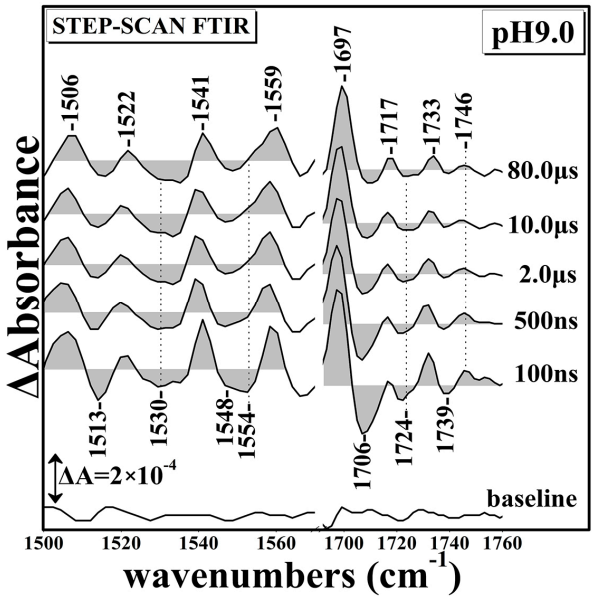

Figure 3. Time Resolved Step-Scan Fourier Transform Infrared (TRS^2-FTIR) difference spectra of 1500–1760 cm^{-1} region (t_d = 100–80,000 ns, 4 cm^{-1} spectral resolution) of fully-reduced ba_3-CO subsequent to CO photolysis by a 7 ns 532 nm laser pulse at pH 9.0.

Figure 4 presents the Time Resolved Step-Scan Fourier Transform Infrared (TRS^2-FTIR) difference spectra of the fully-reduced ba_3-CO complex in D_2O. The experiments were performed in D_2O in order to study the behavior of the protein upon H/D exchange. The amide I band arises 80% from the C=O stretching mode of the amide functional group and 20% from C–N stretching [8–13]. The protein secondary structure consists of a-helix (1648–1660 cm^{-1}), β-sheet (1625–1640 and 1672–1694 cm^{-1}), turns (1660–1685 cm^{-1}), and unordered structures (1640–1650 cm^{-1}) [32,33].

Figure 5 presents the pH sensitivity of Propionate A and aspartic acid residue D372. Features at 1736(+)/1744(−), 1729(−), 1697(+)/1706(−), 1686(+), 1668(+)/1675(−), 1652(+)/1660(−), 1638(+)/1644(−), 1630(−), 1559(+), 1541(+)/1548(−) 1519(−)/1527(−), 1535(−), and 1506(+)/1513(−) at 100 ns, subsequent to CO photolysis, remained unchanged in the t_d = 100–8000 ns range. The 1736(+)/1744(−) and 1729(−) features are slightly pH/pD-dependent since they show small frequency shifts, but the absence of the 1750 cm^{-1} in the pD spectra demonstrates the sensitivity of the protonated form of D372 to pH/pD exchanges. The 1697(+)/1706(−) feature, which has been

attributed to the protonated form of the ring-A propionate, is insensitive to pD exchanges. A group of vibrations at 1668(+)/1675(−) are tentatively assigned to protein turns, those at 1652(+)/1660(−) to α-helical group of vibrations and, finally, those at 1638(+)/1644(−), 1630(−) to β-sheet [29,32]. All of the abovementioned vibrations remained unchanged in the t_d = 100–80,000 ns range. The behavior of all of the vibrational features observed at pD 7 are similar at at pD 6 and pD 9 (Figures S1 and S2).

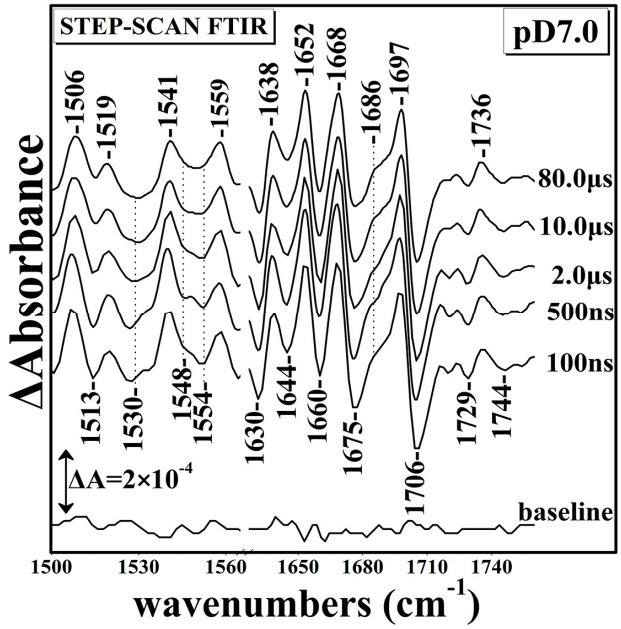

Figure 4. Time Resolved Step-Scan Fourier Transform Infrared (TRS^2-FTIR) difference spectra of 1500–1760 cm^{-1} region (t_d = 100–80,000 ns, 4 cm^{-1} spectral resolution) of fully-reduced ba_3-CO subsequent to CO photolysis by a 7 ns 532 nm laser pulse at pD 7.0.

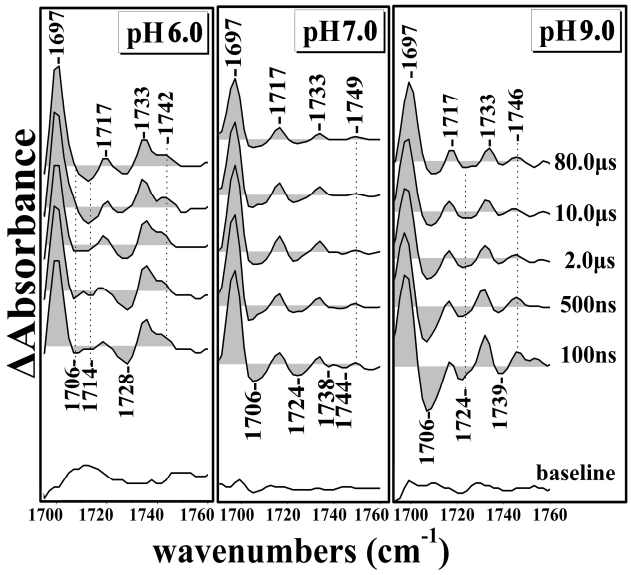

Figure 5. Time Resolved Step-Scan Fourier Transform Infrared (TRS^2-FTIR) difference spectra of 1690–1760 cm^{-1} region (t_d = 100–80,000 ns, 4 cm^{-1} spectral resolution) of fully-reduced ba_3-CO subsequent to CO photolysis by a 7 ns 532 nm laser pulse at pH 6.0, 7.0, and 9.0.

3. Discussion

The Time Resolved Step-Scan FTIR data have already proven to be a very powerful for understanding the transient changes during protein action. The intensity/frequency changes observed in the TRS^2-FTIR difference spectra is the result of the perturbation induced by the photodissociation of CO from heme a_3 and its subsequent binding to Cu_B and to the docking site, which consists of the ring-A propionate heme a_3-D372-H_2O moiety. The presence of protonated/deprotonated forms of D372 and of the ring-A propionate, in association with the dependence of their deprotonated forms on the environment, indicates a protonic connectivity between the D372, the ring-A propionate of heme a_3, and the pair of water molecules w941 and w927. To account for the presence of the observed pH/pD changes and the presence of protonated and deprotonated forms, we present, in Figures 6 and 7, a scheme that includes the ring-A propionate/D372 pair and w927/941. In the oxidative or reductive phase, a proton can be accepted by the ring-A propionate/D372 pair, which influences the release of a proton to the H_2O pool [34–36]. The w941 is not exchangeable; however, it contributes to the dynamics of the ring A-D372-w927. In the scheme, states B and D, in which a single proton is shared between the D372 and the heme a_3 ring A-propionate, can accept a single proton. We propose that this is not operative in the protonated (A) or deprotonated (C) states. We postulate that the observed pH/pD changes in the TRS^2-FTIR data are due to the exchangeable w927 that provides the H-bonded connection in the local moieties of the D372 and ring-A heme a_3 propionate, and has activation energy for proton motion connecting the ligand docking site with the water pool. Consequently, during the formation of the chemical and pumped H^+, the H_2O pool may serve as a primary acceptor for the water molecules. The data reported here indicate that labile protons and w927 are the source of the observed changes to D372, whereas w946-w941-w942, with prop-A-D372 and His-376, form the proton loading site. The observation of $H_2{}^{17}O$ as a product in the reduction of the O_2 reaction near H376, which is located in a complex with several crystallographically-detected H_2O molecules, implies a unique H_2O exit pathway [34]. At this point it should be noted that the mobility of H_2O molecules in hydrophobic cavities makes them undetectable by X-ray crystallography. The ability of D_2O to access the propionate-A-D372 moiety in the pD has been demonstrated by the observed changes to the frequencies of the protonated forms of propionate-A and D372 in the pD 6–9 range. It is suggested that w941/w946 in conjunction with Prop-A-H^+ acts as the Zundel cation that forms the loading proton site (Figures 6 and 7) [18]. In the absence of water molecules in the binuclear center we conclude that the proton loading site is located in the heme a_3 Prop-A-w946-w941w927-D372 moiety [37].

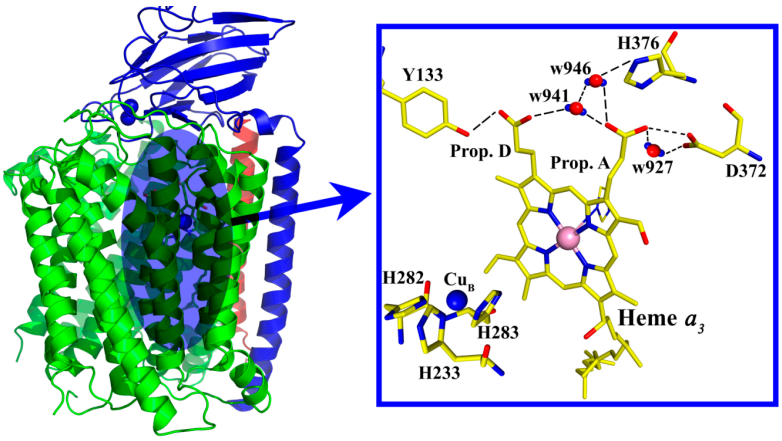

Figure 6. The binuclear heme a_3-Cu_B center and region of the heme a_3 propionates of ba_3 oxidoreductase from *Thermus thermophilus* illustrating the residues of interest [6]. Red, yellow and blue colors represent the oxygen, carbon and nitrogen atoms, respectively. The blue sphere represents the Cu_B atom. In w941, w946 and w927 the red and blue colors represent the oxygen and hydrogen atoms, respectively. The highlighted water molecules are conserved in heme-copper oxidases [18].

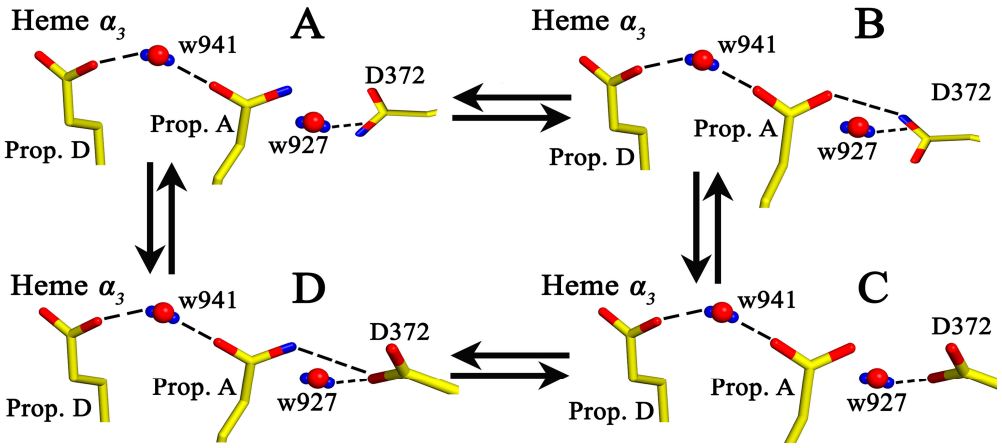

Figure 7. Protonic connectivity between the ring-A propionate of heme a_3, the D372, and the water molecule w927. Blue, red and yellow colors represent protons, oxygen and carbon atoms, respectively. In states **B** and **D**, a single proton is shared between ring-A propionate of heme a_3 and D372, while in state **A**, ring-A propionate of heme a_3 and D372 are protonated and in state **C**, ring-A propionate of heme a_3 and D372 are deprotonated.

4. Materials and Methods

4.1. Sample Preparation

Cytochrome ba_3 was isolated from *Thermus thermophilus* HB8 cells according to previously published procedures. The ba_3 samples were placed in a desired 0.1 M buffer, pH/pD 7.0, HEPES (4-(2-hydroxyethyl) piperazine-1-ethanesulfonic acid), pH/pD 6.0, MES hydrate (2-(*N*-morpholino) ethanesulfonic acid hydrate, 4-morpholineethanesulfonic acid) and pH/pD 9.0, CHES (2-(cyclohexylamino)ethanesulfonic acid). The buffers prepared for the D_2O experiments were measured assuming pD = pH(observed) + 0.4. The concentration of the samples was determined by UV-VIS measurements performed on a Lambda 25 UV-VIS spectrometer (Perkin Elmer, Italy), using $\varepsilon_{416,ox}$ = 152 $mM^{-1} \cdot cm^{-1}$, and was ~700 µM. The fully-reduced CO bound form of the enzyme (ba_3-CO) was prepared by using sodium dithionite as a reducing agent and subsequently exposed to 1 atm of CO under anaerobic conditions. The final samples were transferred to an air-tight, sealed FTIR cell, composed by two CaF_2 windows. The path length was 6 µm for the samples in $H_2{}^{16}O$ and 15 µm for the samples in D_2O. The total enzyme volume used for the experiments was ~1.5 mL. The ^{12}CO gas was obtained from Messer (Germany) and D_2O was purchased from Sigma-Aldrich (Taufkirchen, Germany).

4.2. ns-µs Time-Resolved Step-Scan FTIR Spectroscopy

The ns-µs Time Resolved Step-Scan Fourier Transform Infrared measurements (TRS^2-FTIR) were performed on a Vertex 70 v FTIR spectrometer (Bruker, Karlsruhe, Germany) fitted with a liquid nitrogen-cooled fast Mercury-Cadmium-Telluride (MCT) detector (Figure 8). The optical bench was kept under vacuum conditions and the sample compartment was purged with N_2. The spectral resolution was 4 cm^{-1} and the time resolution was 100 ns. The covered spectral range was 1200–2400 cm^{-1} and an Infrared filter 4200 nm (Spectrogon US INC., Mountain Lakes, NJ, USA) was used. The total number of time slices was 800; 50 of them were taken before the laser triggering and were used as a background reference for the data analysis, and 750 time slices were taken after laser triggering. A 532 nm laser pulse (second harmonic) from a Continuum Minilite Nd-YAG laser (Continuum, San Jose, CA, USA) (7 ns width, 5–8 mJ/pulse, 8 Hz) was used to photolyze the heme a_3-CO complex. Two mirrors were used to direct the 532 nm laser beam inside the spectrometer and through the sample. A Quantum Composers Plus pulse delay generator, Model 9514 (Quantum

Composers Inc., Bozeman Montana, MT, USA) was used to synchronize the spectrometer with the laser. A total of 10 coadditions per retardation data point were collected and 35 measurements of single-sided interferograms were collected and averaged in order to improve the S/N ratio. The AC and DC measurements were taken separately using the same sample. The AC signal was amplified by a factor of two using a Model SR560 Low-Noise preamplifier (Stanford research systems, Sunnyvale, CA, USA). The phase from DC measurements was used for phase correction of the AC measurements. The Blackman–Harris three-term apodization function with 32-cm^{-1} phase resolution and the Mertz/No Peak search phase correction algorithm were used. Difference spectra were calculated using $\Delta A = -\log (I_S/I_R)$.

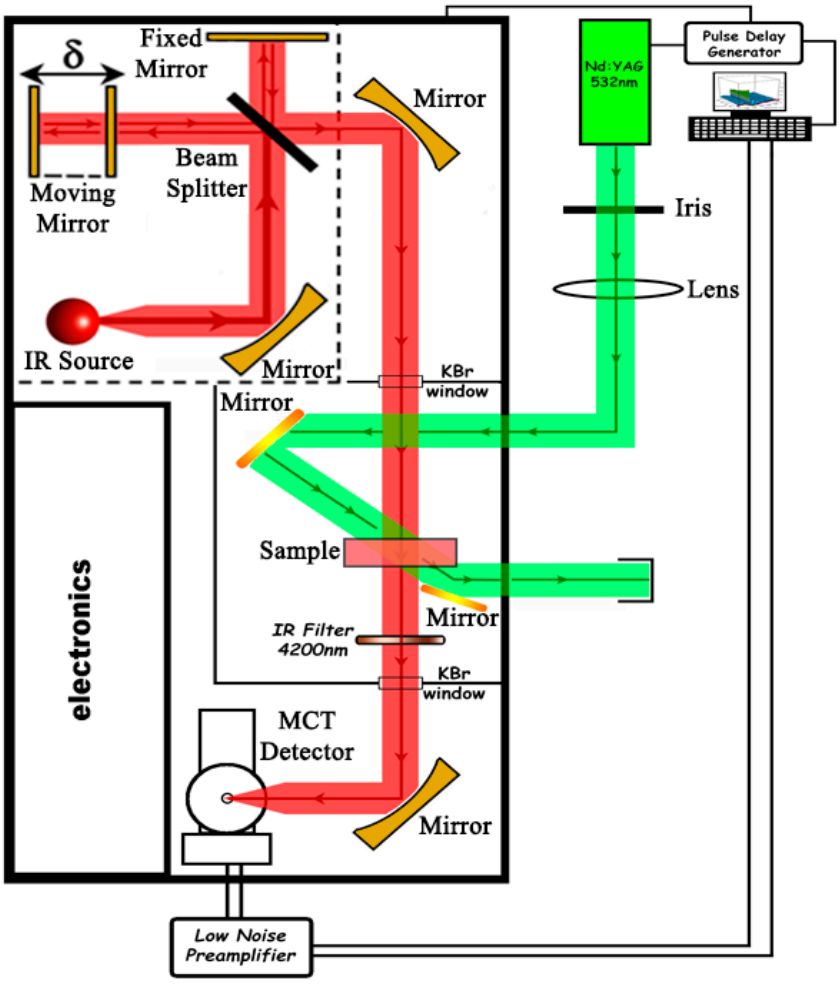

Figure 8. Experimental setup for the ns Time-Resolved Step-Scan Fourier Transform Infrared (ns TRS^2−FTIR). The red and green arrows represent the infrared beam and the 532 nm photolysis beam, respectively.

Supplementary Materials: Supplementary materials can be found at www.mdpi.com/1422-0067/17/10/1657/s1.

Acknowledgments: This work was supported by funds from the Cyprus Research. Promotion Foundation to C.V. (TEXNOLOGIA/THEPIS/0609(BE)/05.

Author Contributions: Antonis Nicolaides performed the experiments and analyzed the data; Tewfik Soulimane provided materials and Constantinos Varotsis wrote the paper.

Conflicts of Interest: The authors declare no conflict of interest.

References

1. Frauenfelder, H.; Sligar, S.G.; Wolynes, P.G. The energy landscapes and motions of proteins. *Science* **1991**, *254*, 1598–1603. [CrossRef] [PubMed]
2. Brzezinski, P.; Gennis, R.B. Cytochrome *c* oxidase: Exciting progress and remaining mysteries. *J. Bioenerg. Biomembr.* **2008**, *40*, 521. [CrossRef] [PubMed]
3. Chang, H.; Choi, S.; Vakkasoglou, A.S.; Chen, Y.; Hemp, J.; Fee, J.A.; Gennis, R.B. Exploring the proton pump and exit pathway for pumped protons in cytochrome ba_3 from *Thermus thermophilus*. *Proc. Natl. Acad. Sci. USA* **2012**, *109*, 5259–5264. [CrossRef] [PubMed]
4. Fee, J.A.; Case, D.A.; Noodleman, L. Toward a chemical mechanism of proton pumping by the B-type cytochrome *c* oxidase: Application of density functional theory to cytochrome ba_3 of *Thermus thermophiles*. *J. Am. Chem. Soc.* **2008**, *130*, 15002. [CrossRef] [PubMed]
5. Wikstrom, M.; Verkhovsky, M.I. Mechanism and energetics of proton translocation by the respiratory heme-copper oxidases. *Biochim. Biophys. Acta* **2007**, *1767*, 1200. [CrossRef] [PubMed]
6. Soulimane, T.; Buse, G.; Bourenkov, G.P.; Bartunik, H.D.; Huber, R.; Than, M.E. Structure and mechanism of the ba_3-cytochrome *c* oxidase from *Thermus thermophiles*. *EMBO J.* **2000**, *19*, 1766. [CrossRef] [PubMed]
7. Koutsoupakis, K.; Stavrakis, S.; Pinakoulaki, E.; Soulimane, T.; Varotsis, C. Observation of the equilibrium Cu_B-CO complex and functional implications of the transient heme a_3 propionates in cytochrome ba_3-CO from *Thermus thermophilus*. *J. Biol. Chem.* **2002**, *277*, 32860–32866. [CrossRef] [PubMed]
8. Koutsoupakis, C.; Soulimane, T.; Varotsis, C. Docking site dynamics of ba_3-cytochrome *c* oxidase from *Thermus thermophiles*. *J. Biol. Chem.* **2003**, *278*, 36806–36809. [CrossRef] [PubMed]
9. Koutsoupakis, C.; Soulimane, T.; Varotsis, C. Ligand binding in a docking site of cytochrome *c* oxidase: A time-resolved step-scan fourier transform infrared study. *J. Am. Chem. Soc.* **2003**, *125*, 14728–14732. [CrossRef] [PubMed]
10. Porrini, M.; Daskalakis, V.; Farantos, S.; Varotsis, C. Heme cavity dynamics of photodissociated CO from ba_3-cytochrome c oxidase: The role of ring-D propionate. *J. Phys. Chem. B* **2009**, *112*, 12129–12135. [CrossRef] [PubMed]
11. Koutsoupakis, C.; Soulimane, T.; Varotsis, C. Probing the Q-Proton pathway of ba_3-cytochrome *c* oxidase by time-resolved fourier transform infrared spectroscopy. *Biophys. J.* **2004**, *86*, 2438–2444. [CrossRef]
12. Koutsoupakis, K.; Stavrakis, S.; Soulimane, T.; Varotsis, C. Oxygen-linked equilibrium Cu_B-CO species in Cytochrome ba_3 oxidase from *Thermus Thermophilus*: Implications for an oxygen channel at the Cu_B site. *J. Biol. Chem.* **2003**, *278*, 14893–14896. [CrossRef] [PubMed]
13. Koutsoupakis, C.; Soulimane, T.; Varotsis, C. Spectroscopic and kinetic investigation of the fully reduced and mixed valence states of ba_3-Cytochrome *c* Oxidase from *Thermus thermophilus*. *J. Biol. Chem.* **2012**, *287*, 37495–37507. [CrossRef] [PubMed]
14. Pinakoulaki, E.; Ohta, T.; Soulimane, T.; Kitagawa, T.; Varotsis, C. Detection of the His-Heme Fe^{2+} -NO Species in the Reduction of NO to N_2O by ba_3-Oxidase from *Thermus thermophilus*. *J. Am. Chem. Soc.* **2005**, *127*, 15161–15167. [CrossRef] [PubMed]
15. Koutsoupakis, C.; Kolaj-Robin, O.; Soulimane, T.; Varotsis, C. Probing protonation/deprotonation of tyrosine residues in cytochrome ba_3 oxidase from *Thermus thermophilus* by time-resolved step-scan FTIR spectroscopy. *J. Biol. Chem.* **2011**, *286*, 30600–30605. [CrossRef] [PubMed]
16. Koutsoupakis, C.; Pinakoulaki, E.; Stavrakis, S.; Daskalakis, V.; Varotsis, C. Time-resolved step-scan Fourier transform infrared investigation of heme-copper oxidases: Implications for O_2 input and H_2O/H^+ output channels. *Biochim. Biophys. Acta Bioenerg.* **2004**, *1655*, 347–352. [CrossRef] [PubMed]
17. Daskalakis, V.; Varotsis, C. Binding and docking interactions of NO, CO and O_2 in heme proteins as probed by density functional theory. *Int. J. Mol. Sci.* **2009**, *10*, 4137–4156. [CrossRef] [PubMed]
18. Nicolaides, A.; Soulimane, T.; Varotsis, C. Detection of functional hydrogen-bonded water molecules with protonated/deprotonated key carboxyl side chains in the respiratory enzyme ba_3-oxidoreductase. *Phys. Chem. Chem. Phys.* **2015**, *17*, 8113–8119. [CrossRef] [PubMed]
19. Daskalakis, V.; Farantos, S.C.; Guallar, V.; Varotsis, C. Regulation of electron and proton transfer by the protein matrix of Cytochrome c Oxidase. *J. Phys. Chem. B* **2011**, *115*, 3648–3655. [CrossRef] [PubMed]
20. Koutsoupakis, C.; Soulimane, T.; Varotsis, C. Photobiochemical production of carbon monoxide by thermus thermophilus ba_3-Cytochrome *c* oxidase. *Chem. Eur. J.* **2015**, *21*, 4958–4961. [CrossRef] [PubMed]

21. Loullis, A.; Noor, M.R.; Soulimane, T.; Pinakoulaki, E. The structure of a ferrous heme-nitro species in the binuclear a_3/Cu_B center of ba_3-cytochrome c oxidase as determined by resonance Raman spectroscopy. *Chem. Commun.* **2015**, *51*, 286–289. [CrossRef] [PubMed]
22. Loullis, A.; Noor, M.R.; Soulimane, T.; Pinakoulaki, E. Observation of Ligand Transfer in ba_3 Oxidase from *Thermus thermophilus*: Simultaneous FTIR detection of photolabile heme $a_3{}^{2+}$–CN and transient $Cu_B{}^{2+}$–CN complexes. *J. Phys. Chem. B* **2012**, *116*, 8955–8960. [CrossRef] [PubMed]
23. Nicolaides, A.; Soulimane, T.; Varotsis, C. Nanosecond ligand migration and functional protein relaxation in ba_3 oxidoreductase: Structures of the B0, B1 and B2 intermediate states. *Biochim. Biophys. Acta* **2016**, *1857*, 1534–1540. [CrossRef] [PubMed]
24. Pinakoulaki, E.; Varotsis, C. Resonance Raman spectroscopy of nitric oxide reductase and cbb_3 heme-copper oxidase. *J. Phys. Chem. B* **2008**, *112*, 1851–1857. [CrossRef] [PubMed]
25. Pinakoulaki, E.; Varotsis, C. Time-resolved resonance raman and time-resolved step-scan FTIR studies of nitric oxide reductase from *Paracoccus denitrificans*: Comparison of the heme b_3-Fe site to that of the Heme-Cu_B in oxidases. *Biochemistry* **2003**, *42*, 14856–14861. [CrossRef] [PubMed]
26. Pinakoulaki, E.; Yoshimura, H.; Yoshioka, S.; Aono, S.; Varotsis, C. Recognition and discrimination of gases by the oxygen-sensing signal transducer protein HemAT. *Biochemistry* **2006**, *45*, 7763–7766. [CrossRef] [PubMed]
27. Lambrou, A.; Pinakoulaki, E. Resonance Raman detection of the myoglobin nitrito heme Fe-O-N=O/2-nitrovinyl species: Implications for Helix E-Helix F interactions. *Phys. Chem. Chem. Phys.* **2015**, *17*, 3841–3849. [CrossRef] [PubMed]
28. Tomson, F.; Bailey, J.A.; Gennis, R.B.; Unkefer, C.J.; Li, Z.; Silks, L.A.; Martinez, R.A.; Donohoe, R.J.; Dyer, R.B.; Woodruff, W.H. Direct infrared detection of the covalently ring linked His−Tyr structure in the active site of the Heme−Copper Oxidases. *Biochemistry* **2002**, *41*, 14383–14390. [CrossRef] [PubMed]
29. Rich, P.; Maréchal, A. Carboxyl group functions in the heme-copper oxidases: Information from mid-IR vibrational spectroscopy. *Biochim. Biophys. Acta* **2008**, *1777*, 912–918. [CrossRef] [PubMed]
30. Heitbrink, D.; Sigurdson, H.; Bolwien, C.; Brzezinski, P.; Heberle, J. Transient binding of CO to Cu_B in cytochrome *c* Oxidase is dynamically linked to structural changes around a carboxyl group: A time-resolved step-scan fourier transform infrared investigation. *Biophys. J.* **2002**, *82*, 1–10. [CrossRef]
31. Kandori, H.; Nakamura, H.; Yamazaki, Y.; Mogi, T. Redox-induced protein structural changes in cytochrome *bo* revealed by fourier transform infrared spectroscopy and [^{13}C] Tyr labeling. *J. Biol. Chem.* **2005**, *280*, 32821–32826. [CrossRef] [PubMed]
32. Barth, A. Infrared spectroscopy of proteins. *Biochim. Biophys. Acta* **2007**, *1767*, 1073–1101.
33. Hellwig, P.; Soulimane, T.; Buse, G.; Mantele, W. Electrochemical, FTIR, and UV/VIS spectroscopic properties of the ba_3 oxidase from *Thermus thermophilus*. *Biochemistry* **1999**, *38*, 9648–9658. [CrossRef] [PubMed]
34. Branden, G.; Branden, M.; Schmidt, B.; Mills, D.A.; Ferguson-Miller, S.; Brzezinski, P. The protonation state of a heme propionate controls electron transfer in cytochrome *c* oxidase. *Biochemistry* **2005**, *44*, 10466–10474. [CrossRef] [PubMed]
35. Von Balmoos, C.; Gonska, N.; Lachmann, P.; Gennis, R.B.; Ädelroth, P.; Brzezinski, P. Mutation of a single residue in the ba_3 oxidase specifically impairs protonation of the pump site. *Proc. Natl. Acad. Sci. USA* **2015**, *1012*, 3397–3402. [CrossRef] [PubMed]
36. Lu, J.; Gunner, M.R. Characterizing the proton loading site in cytochrome *c* oxidase. *Proc. Natl. Acad. Sci. USA* **2014**, *102*, 12414–12419. [CrossRef] [PubMed]
37. Einarsdóttir, O.; McDonald, W.; Funatogawa, W.; Szundi, I.; Woodruff, W.H.; Dyer, R.B. The pathway of O_2 to the active site in heme-copper oxidases. *Biochim. Biophys. Acta* **2015**, *1847*, 109–118. [CrossRef] [PubMed]